
# Investigation of Main Injection Quantity Fluctuation due to Pilot Injection in High Pressure Common Rail Fuel Injection System

Tian Bingqi, Fan Liyun*, Ma Xiuzhen, Qaisar Hayat, Bai Yun, Liu Yang
School of Power and Energy Engineering, Harbin Engineering University, Harbin, China
*Corresponding author: fanly_01@163.com

***Submitted: Jan. 18, 2014*** ***Accepted: Apr. 24, 2014*** ***Published: June 1, 2014***

***Abstract- High pressure common rail (HPCR) fuel injection system is the main development trend for fuel injection system of diesel engine. Precise controlling of injection pressure and multiple injections are the advantages and key features of the HPCR system. Affect of pilot injection quantity (PIQ) and pilot-main interval (PMI) on main injection quantity fluctuation (MIQF) has been investigated in this paper by evaluating performance coherence and stability of injection quantity of diesel engine. A numerical model of HPCR system has been development in AMESim environment. Predicting accuracy of the numerical model has been validated by comparing its results with experimental data. The results show that the pilot injection triggers pressure cyclical fluctuation in the electro-injection delivery chamber and gives rise to MIQF. Amplitude of MIQF decreases with increase of PMI and increase with increase of PIQ. Moreover, variation of PIQ has also influence on both the amplitude and the phase of MIQF. Influence of MIQ on amplitude of MIQF depends on how many pressure fluctuation cycles have been incorporated in the main injection.***

**Index terms*:* High pressure common rail, Numerical model, Pilot-main injection, Main injection quantity, Pilot-main interval.**

# I. INTRODUCTION

Gradual decreasingly of petroleum resources and increasingly strict emission regulations have pushed researchers to develop better diesel engines and their injection system [1, 2]. High pressure common rail (HPCR) fuel injection system can optimize combustion process, reduce $NO_X$, specific fuel consumption and noise effectively by adjusting injection pressure independent from engine rotational speed and implements a flexible regulation of injection timing, duration and rate [3].

The pilot-main injection regulated by the HPCR system is an effective method for improving diesel engine's performance [4, 5]. Fuel injected during pilot injection ahead of the main injection enhances cold start performance by shortening the ignition delay period of fuel injected during main injection. It also cuts down combustion temperature, $NO_X$ emission, combustion noise and vibration by decreasing premixed combustion, reducing rate of heat release and pressure rise [6, 7]. Su Han Park has investigated the effects of multiple-injection on spray behavior, combustion and emission. He has concluded that the pilot-main injection can improve indicated mean effective pressure and cut down the emissions of soot, HC and CO [8]. F.Payri has studied the influence of pilot-main injection mode during idling after cold start of diesel engines. His results show that an appropriate pilot timing can promote adequate in-cylinder conditions for the main combustion [9]. G. M. Bianchi has investigated the effect of multiple injections on emissions of a common rail injection system and concluded that the multiple injection strategy is effective in reducing $NO_X$ and soot [10].

However the main injection quantity (MIQ) fluctuates with variation of pilot injection quantity (PIQ) and pilot-main interval (PMI). As a result coherence and stability of injection worsens and deteriorates the performance of diesel engine. So it is necessary to study the injection characteristics of pilot-main injection, analysis the causes of main injection quantity fluctuation (MIQF) and the influence mechanism of pilot injection on main injection for controlling stability of the MIQ.

Mirko Baratta has studied the influence of high pressure supply pipe of injector on stability of multiple-injection. The results show that by shortening the length and increasing the inner diameter of the high pressure supply pipe of injector, the amplitude of pressure fluctuation can be reduced and the frequency of pressure fluctuation can be increased during multiple-injection.

Influence of pressure fluctuation triggered by variation of PMI on subsequent injection quantity can be reduced through orifice installed between the common rail and high pressure supply pipe of injector [11].

In present paper a numerical model has been developed in AMESim environment for simulating the injection characteristics of HPCR system. The prediction accuracy of the model is verified by comparing the simulated results to experimental results obtained from HPCR system test bench. The variation law of MIQF caused by PIQ and PMI is obtained and the reason for MIQF and its influence mechanism has been determined. The conclusions of this paper can be utilized for correcting MIQ in pilot-main injection control in order to improve the stability of pilot-main injection process. Fig.1 represents the functional block diagram of research work of this paper.

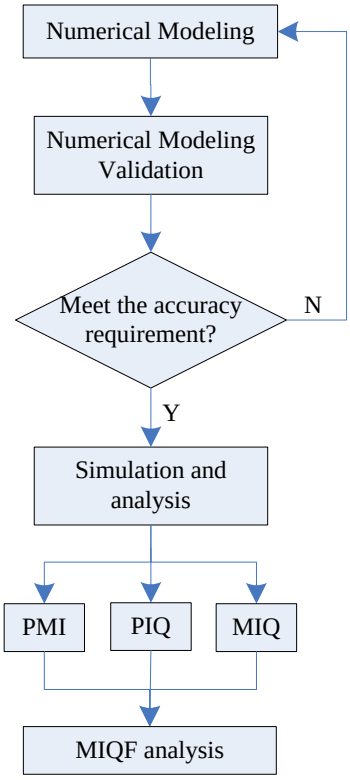


Figure 1. Research flowchart

Rest of this paper is organized as follows. Operation principle of HPCR system is described in section II. Numerical model of HPCR system which consists of supply pump, fuel metering valve, high pressure pump, common rail, injector and ECU is developed and validation of numerical model is presented in section III. Whereas simulated results of MIQF with different PIQ, MIQ and PMI are analyzed in detail in Section IV. Conclusions are made in Section V.

## II. OPERATION PRINCIPLE OF HPCR SYSTEM

As shown in Fig.2, HPCR system mainly consists a low pressure circuit including supply pump and fuel tank, a high pressure pump with a fuel metering valve, a common rail with pressure limited valve, several electro-injectors, an electronic control unit (ECU) and several sensors [12, 13].

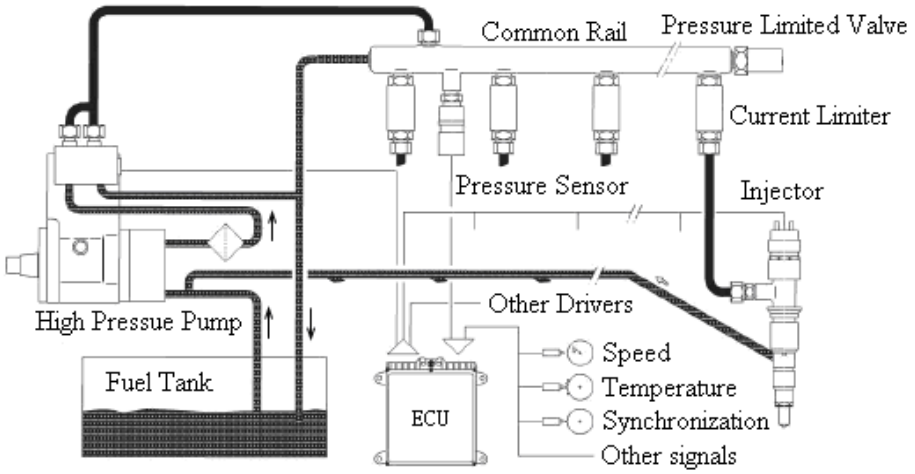


Figure 2. Schematic of the HPCR system

Fuel in tank is delivered to high pressure pump and then filled into common rail. Fuel supply volume is determined by a metering valve installed on high pressure pump and controlled by ECU according to the pressure deviation between actual rail pressure and target rail pressure. The common rail maintains high pressure and supplies fuel to electro-injectors for injection. Main elements of an electro-injector are a solenoid including electromagnet, armature and control valve, a hydraulic servo mechanism with inlet orifice, outlet orifice, control chamber, control piston, a nozzle with needle and delivery chamber. The ECU sends commands to metering valve and electro-injector in order to regulate rail pressure by adjusting metering valve's opening and governing injection timing, duration and rate are adjusted by controlling the opening time, duration and timing of solenoid according to state signals received from sensors.

## III. SIMULATION MODEL AND BENCH TEST

CR system is a complex system in which different fields such as electric, magnetic, mechanical movement and flow are coupled together [14]. The interactions between these fields are complicated and hence it is necessary to use a combination method including simulations and experiments to investigate injection characteristics of HPCR system. The HPCR system can be described by suitably combining the continuity and motion equations fro different fields such as electric, magnetic, mechanical movement and flow are coupled together by control equations.

The continuity equation of plunger chamber can be written as follow [15, 16]

$$\frac{dP_p}{dt} = \frac{a^2 \rho}{V_p}\left[ S_p \frac{dh_p}{dt} - Q_{pr} - Q_{p-leak} \right] \tag{1}$$

With,

$$Q_{pr} = \mu_{pr} A_{pr} \sqrt{\frac{2}{\rho}\left|P_p - P_r\right|} \tag{2}$$

$$Q_{p-leak} = \frac{\pi d_p \delta_p^3 \left(P_p - P_0\right)}{12 \eta l_p} \tag{3}$$

Where $P_p$ is pressure in plunger chamber, $a$ is sonic velocity, $\rho$ is density of fuel, $V_p$ is volume of plunger chamber determined by plunger lift, $S_p$ is plunger cross section, $hp$ is plunger lift, $Q_{pr}$ is the flow rate from pump to rail, $Q_{p\text{-}leak}$ is the flow rate from pump to tank via the clearance between plunger and plunger sleeve, $\mu_{pr}$ is flow coefficient between pump to rail, $A_{pr}$ is flow area from pump to rail, $P_p$ is pressure in plunger chamber, $P_r$ is rail pressure, $d_p$ is plunger diameter, $\delta_p$ is clearance between plunger and plunger sleeve, $P_0$ is tank pressure, $\eta$ is kinetic viscosity of fuel, $l_p$ is length of the clearance between plunger and plunger sleeve.

The continuity equation of common rail is:

$$\frac{dP_r}{dt} = \frac{a^2 \rho}{V_r}\left[ \sum Q_{pr} - \sum \left( Q_{rd} + Q_{rc} \right) \right] \tag{4}$$

With,

$$Q_{rd} = \mu_{rd} A_{rd} \sqrt{\frac{2}{\rho}\left|P_r - P_d\right|} \tag{5}$$

$$Q_{rc} = \mu_{rc} A_{rc} \sqrt{\frac{2}{\rho}\left|P_r - P_c\right|} \tag{6}$$

Where $V_r$ is volume of common rail, $Q_{rd}$ is the flow rate from rail to delivery chamber, $Q_{rc}$ is the flow rate from rail to control chamber, $\mu_{rd}$ and $A_{rd}$ are flow coefficient and flow area from rail to delivery chamber respectively, $P_d$ is pressure in delivery chamber, $\mu_{rc}$ and $A_{rc}$ are flow coefficient and flow area from rail to control chamber respectively, $P_c$ is pressure in control chamber.

The continuity equation of injector delivery chamber is [17-19]:

$$\frac{dP_d}{dt} = \frac{a^2 \rho}{V_d}\left[ Q_{rd} - S_n \frac{dh_n}{dt} - Q_{dcyl} - Q_{n-leak} \right] \tag{7}$$

With,

$$Q_{dcyl} = \mu_{dcyl} A_{dcyl} \sqrt{\frac{2}{\rho}\left|P_d - P_{cyl}\right|} \tag{8}$$

$$Q_{n-leak} = \frac{\pi d_n \delta_n^3 \left(P_d - P_0\right)}{12 \eta l_n} \tag{9}$$

Where $V_d$ is volume of delivery chamber varies with movement of needle, $S_n$ is needle cross section, $h_n$ is needle lift, $Q_{dcyl}$ is the flow rate from delivery chamber to cylinder, $Q_{n\text{-}leak}$ is the flow rate from delivery chamber to tank via the clearance between needle and needle sleeve, $\mu_{dcyl}$ and $A_{dcyl}$ are flow coefficient and flow area from delivery chamber to cylinder respectively, $P_{cyl}$ is pressure in cylinder, $d_n$ is needle diameter, $\delta_n$ is clearance between needle and needle sleeve, $l_n$ is length of clearance between needle and needle sleeve.

The continuity equation of injector control chamber is:

$$\frac{dP_c}{dt} = \frac{a^2 \rho}{V_c}\left[ Q_{rc} + S_{cp} \frac{dh_{cp}}{dt} - Q_{ct} - Q_{cp-leak} \right] \tag{10}$$

With,

$$Q_{ct} = \mu_{ct} A_{ct} \sqrt{\frac{2}{\rho}\left|P_c - P_0\right|} \tag{11}$$

$$Q_{cp-leak} = \frac{\pi d_{cp} \delta_{cp}^3 \left(P_c - P_0\right)}{12 \eta l_{cp}} \tag{12}$$

Where $V_c$ is volume of control chamber determined by lift of control piston, $S_{cp}$ is cross section of control piston, $h_{cp}$ is control piston lift, $Q_{ct}$ is the flow rate from control chamber to tank, $Q_{cp\text{-}leak}$ is

the flow rate from control chamber to tank via the clearance between control piston and control piston sleeve, $\mu_{ct}$ and $A_{ct}$ are flow coefficient and flow area from control chamber to tank respectively, $d_{cp}$ is control piston diameter, $\delta_{cp}$ is clearance between control piston and control piston sleeve, $l_{cp}$ is length of the clearance between control piston and control piston sleeve.

The motion equation of control valve is [20]:

$$m_{cv}\frac{d^2h_{cv}}{dt^2} = F_{mag} - F_{hyd} - k_{cv}(h_{cv} + h_{cv0}) \tag{13}$$

Where $m_{cv}$ is mass of control valve, $h_{cv}$ is control valve lift, $F_{mag}$ is magnetic force engerdered by solenoid, $F_{hyd}$ is hydraulic force imposed on control valve, $k_{cv}$ is stiffness of control valve spring, $h_{cv0}$ is pre-compression of control valve spring.

The motion equation of needle and control piston is:

$$m\frac{d^2h_n}{dt^2} = S_n\left(P_d - P_{cyl}\right) - S_{cp}\left(P_c - P_0\right) - k_n(h_n + h_{n0}) \tag{14}$$

Where $m$ is mass of needle and control piston, $k_n$ is stiffness of needle spring, $h_{n0}$ is pre-compression of needle spring.

The wave equation in fuel pipe is [21, 22]:

$$\frac{\partial u}{\partial x} + \frac{1}{a^2\rho}\frac{\partial p}{\partial t} + \frac{u}{a^2\rho}\frac{\partial p}{\partial x} = 0 \tag{15}$$

$$\rho\left(\frac{\partial u}{\partial t} + u\frac{\partial u}{\partial x}\right) + \frac{\partial p}{\partial x} + 2\lambda_f\rho u = 0 \tag{16}$$

Where $u$ is fuel flow velocity, $\lambda_f$ is coefficient of flow resistance.

Based on the structure principle and equations 1-16 of HPCR system, a simulation model with supply pump, fuel metering valve, high pressure supply pump, common rail, injector and ECU etc has been developed in AMESim environment as shown in Fig.3 [23]. Table 1 presents the main parameters of the HPCR system.

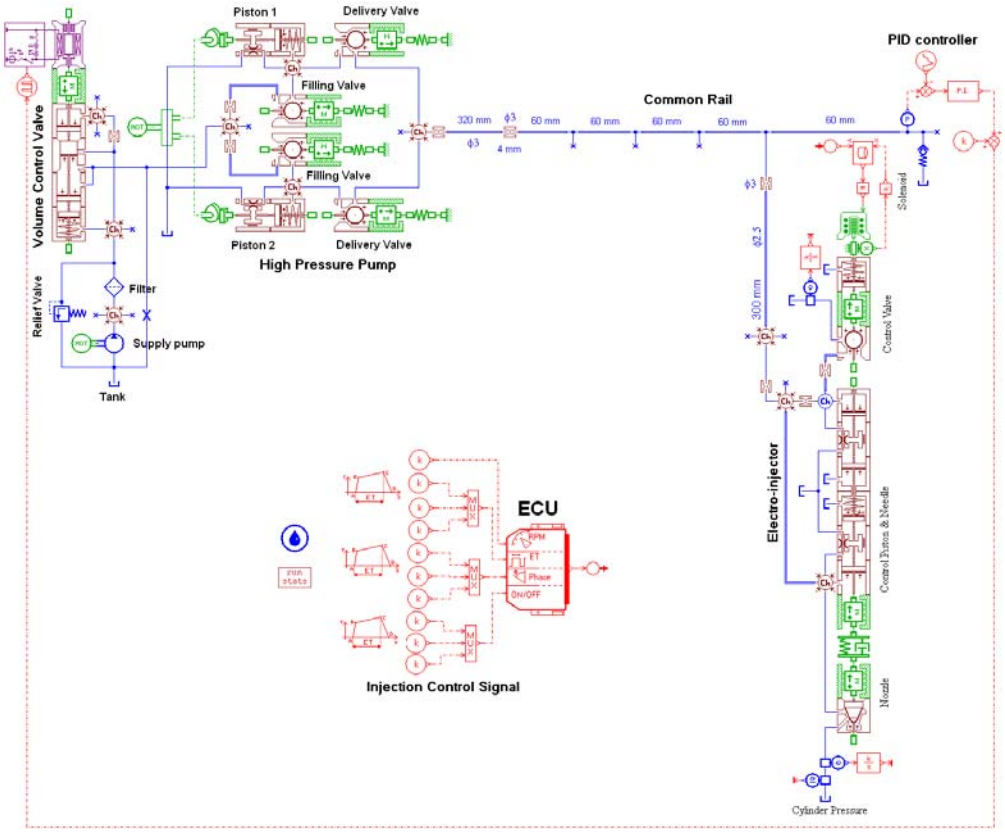


Figure 3. AMESim simulation model of the HPCR system

Table 1: Main parameters of CR system

| Component | Parameter | Value |
|---|---|---|
| Supply pump | Supply rate of supply pump | 5L/min |
| | Relife valve open pressure | 0.4MPa |
| High pressure pump | Plunger diameter | 6mm |
| | Cam lift | 9mm |
| Common rail | Common rail inner diameter | 9.5mm |
| | Common rail volume | 21.5ml |
| | Limited valve open pressure | 220MPa |
| High pressure pipe | Length (pump to rail) | 320mm |
| | Inner diameter (pump to rail) | 3mm |
| | Length (rail to injector) | 300mm |
| | Inner diameter (rail to injector) | 2.5mm |
| Injector | Control valve lift | 0.08mm |
| | Diameter of inlet orifice | 0.24mm |
| | Diameter of outlet orifice | 0.27mm |
| | Needle lift | 0.3mm |

The HPCR test bench equipped with HPCR system produced by Bosch is shown in Fig.4, with a high pressure pump driven by a motor, a common rail and an injector. During the experiments rail pressure was measured by Kistler 4067 high pressure sensor. Fuel injection rate of electro-injector was measured by EFS 8246 module and injection control current signal was measured by DL750 Scope recorder. In order to obtain the same rail pressure characteristics as actual system with four cylinders, the electro-injector controlled by EFS 8233 module injects four times in each cycle during experiment.

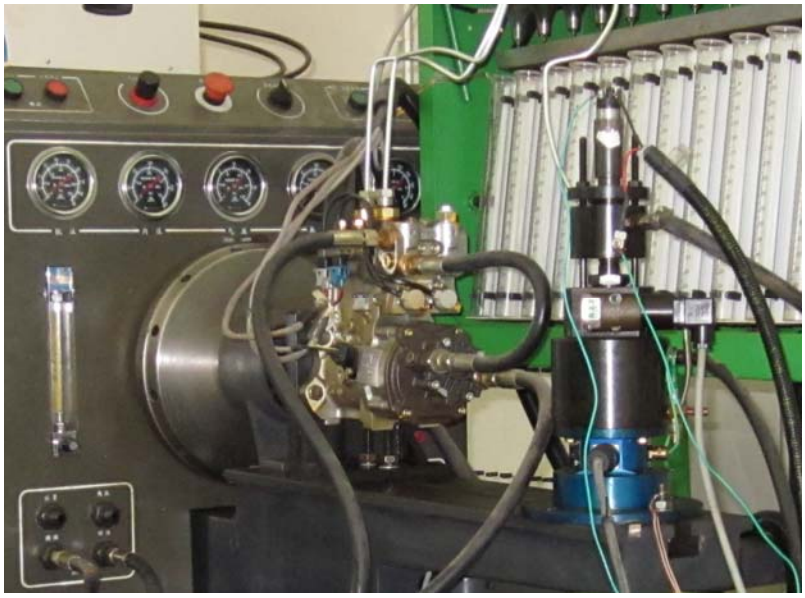

Figure 4. Experiment test bench of HPCR system

Fig.5 and 6 are the comparison curves of rail pressure and injection rate obtained by experiment and simulation with 750r/min pump shaft speed, 135MPa rail pressure and 1.2ms injection duration. The electro-injector in both test bench and simulation model injects four times during every revolution. It is clear from the figures that the frequency and oscillation amplitude of rail pressure in experiment and simulation have a good consistency. Moreover, the model can also accurately predict injection rate in both time sequence and value.

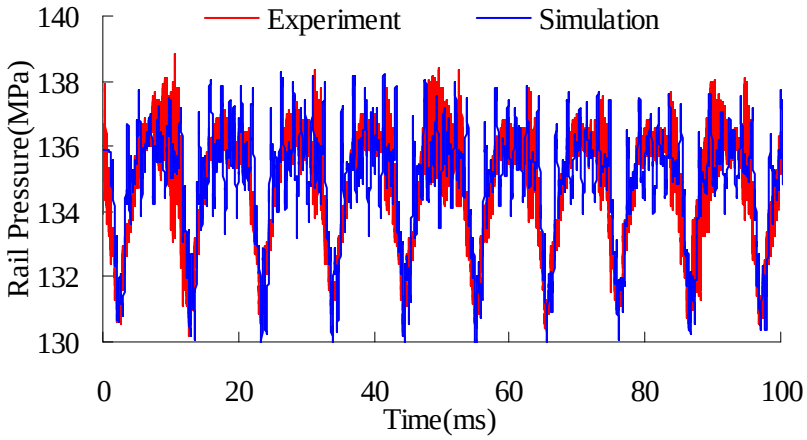


Figure 5. Comparison curve of rail pressure

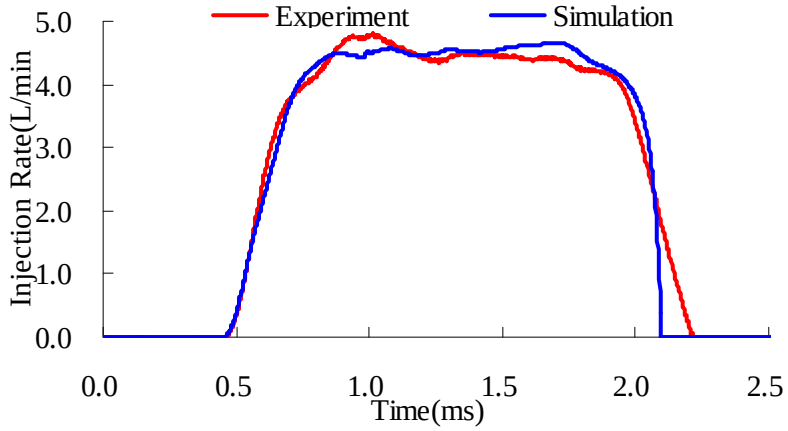


Figure 6. Comparison curve of injection rate

## IV. IMPACT OF PILOT INJIETION ON MAIN INJECTION QUANTITY FLUCTUATION

Though the HPCR system can regulate cycle fuel injection quantity of single injection accurately, but the MIQ in pilot-main injection fluctuates with different PIQ and PMI.

Numerical results of the impact of PIQ on MIQ at varying PMI in pilot-main injection are shown in Fig 7. It is clear from the figure that MIQ changes with PMI at PIQ of $1mm^3$, $6mm^3$, $12mm^3$ and $18mm^3$ PIQ under 750r/min pump shaft speed (1500r/min engine speed), 120MPa rail pressure and $60mm^3$ MIQ pilot-main injection operating conditions. Because the pilot and main injection of pilot-main injection with $18mm^3$ PIQ are merged together when the PMI is smaller than 0.2ms, only the MIQ with PMI larger than 0.2ms has been plotted in Fig.7.

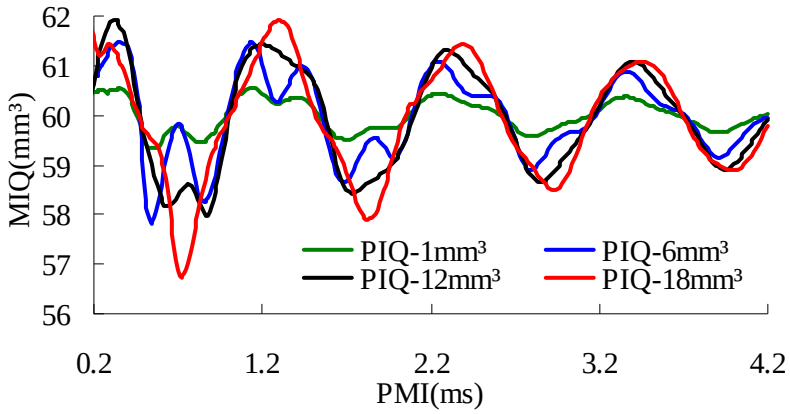


Figure 7. MIQ with different PIQ in pilot-main injection

It can be seen that after pilot injection the MIQ presents cyclical fluctuation with PMI and the amplitude of it declines with increase of PMI. With increase of the PIQ, the amplitude of MIQ fluctuation rises and the phase is delayed. The MIQ fluctuation cycle is 1.1ms and has no obvious change with both increase of PMI and PIQ. The maximum MIQF is -3.28mm$^3$ with 18 mm$^3$ PIQ and 0.72ms PMI.

Fig.8 is fuel pressure in electro-injector delivery chamber (Pd) and pilot injection rate (IR) with 1mm$^3$, 6mm$^3$, 12mm$^3$ and 18mm$^3$ PIQ respectively and no main injection. As shown in Fig.8, the injection induces pressure drop in delivery chamber as soon as the pilot injection is starting and pressure fluctuates cyclically with time even after the pilot injection has finished. The amplitude of fluctuation declines with the increase of time. That is why the MIQ fluctuates with change of PMI and the amplitude decreases with increase of PMI. While the fluctuation amplitude of the pressure increases and the phase is postponed with increase of PIQ. The reason is that the larger PIQ will induce more obvious pressure drop and has to take much longer time for completing injection then postpones the fluctuation of pressure in delivery chamber after injection as shown in Fig.8. Pressure fluctuation cycle caused by pilot injection has no change with both PIQ and PMI because it is determined by the structure of HPCR system.

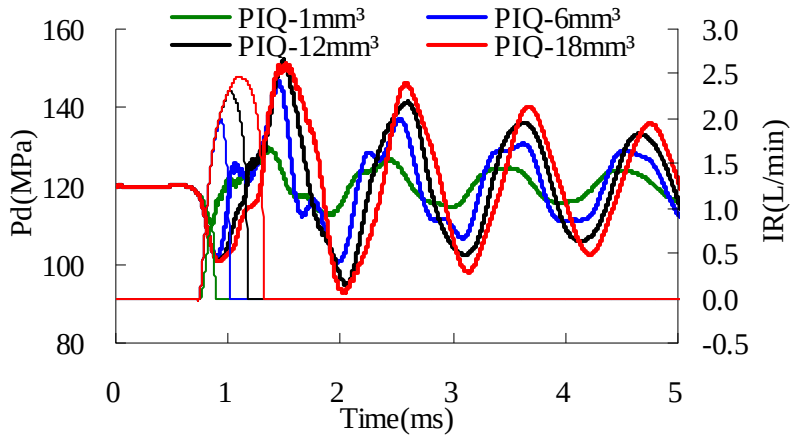


Figure 8. Delivery chamber pressure and injection rate with different PIQ and no main injection

Fig.9 is the MIQF caused by 12mm$^3$ PIQ with 15mm$^3$, 30mm$^3$, 60mm$^3$ and 120mm$^3$ MIQ in pilot-main injection. As the pilot and main injections are merged together when PMI is smaller than 0.12ms with 12mm$^3$ PIQ; therefore only the MIQF with PMI values larger than 0.12ms have been taken into consideration.

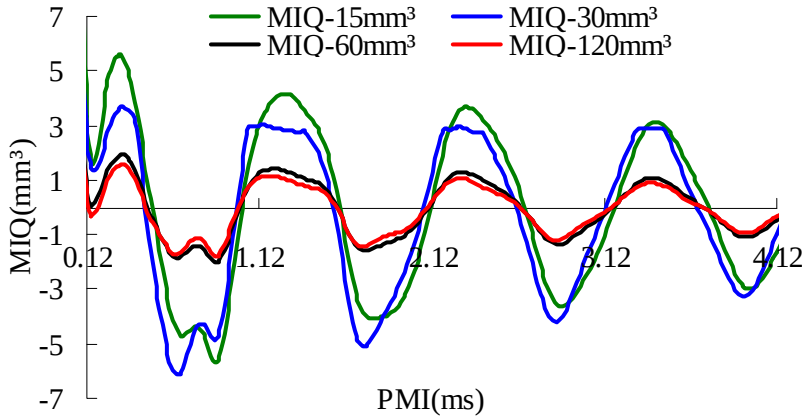


Figure 9. MIQF with different MIQ caused by the 12mm$^3$ PIQ

From Fig.9 it is clear that MIQF is different with different MIQ in pilot-main injection even through the PIQ is same. The MIQF decreases with increase of PMI because the amplitude of pressure fluctuation drops with increase of PMI. The MIQF has large change rate when the MIQ increases from 15mm$^3$ to 60mm$^3$. But when the MIQ increases from 60mm$^3$ to 120mm$^3$, the MIQF

has no obvious change. The cycle of MIQF has no change with different MIQ. The largest MIQF of 5.62mm$^3$ is obtained with 15mm$^3$ MIQ and 0.32ms PMI.

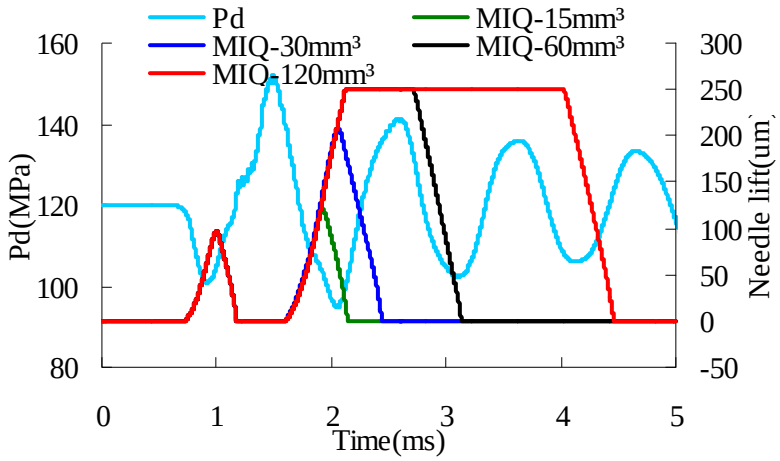


Figure 10. Delivery chamber pressure with 12mm$^3$ single injection quantity and needle lift in pilot-main injection

Fig.10 shows the delivery chamber pressure fluctuation triggered by single injection with 12mm$^3$ PIQ and the needle lift with at PIQ of 12mm$^3$ and MIQ of 15mm$^3$, 30mm$^3$, 60mm$^3$, 120mm$^3$ respectively. It can be seen that the pilot injection and the timing of main injection are the same in the four pilot-main injection processes. It means that the pressure conditions are the same when main injections are starting. So the reason for the amplitude of MIQF changes with different MIQ is how many pressure fluctuation cycles have been incorporated in the main injection duration.

As shown in Fig.10 the main injection durations of MIQ with 15mm$^3$ and 30mm$^3$ are less than one pressure fluctuation cycle. MIQs larger than main injection duration have very less pressure fluctuations when compared to MIQs less than main injection duration. MIQF of 60mm$^3$ and 120mm$^3$ MIQ is smaller than 15mm$^3$ and 30mm$^3$ MIQ. Therefore pressure fluctuation depends on PMI and MIQ. Not only the starting injection pressure of the two main injections is same, but also the pressure in the end of injection is similar; therefore the MIQF with 60mm$^3$ and 120mm$^3$ MIQ is similar.

## V. CONCLUSIONS

A numerical model of HPCR system has been developed in AMESim environment and validated by experiments. The comparison results show that the numerical model can predict injection characteristics of HPCR system accurately. The pressure cyclical fluctuation in the electro-injector delivery chamber triggered by pilot injection in pilot-main injection will cause MIQF. Effect of PIQ, MIQ and PMI on MIQF caused by pilot injection has been analyzed. The MIQF increases with increase of PIQ and decreases with increase of PMI. Variation of PIQ in pilot-main injection not only has influence on the amplitude of MIQF but also has impact on the phase of MIQF. With increase of PIQ the phase of MIQF is delayed. The effect of MIQ on MIQF caused by pilot injection is determined by how many pressure fluctuation cycles have been incorporated in the main injection duration. The cycle of MIQF is determined by the structure of HPCR system and has no change with variation of PIQ, PMI and MIQ.

## VI. ACKNOWLEDGMENT

This work is supported by the National Natural Science Foundation of China [grant number NSFC 51279037&50909024], the Program for New Century Excellent Talents in University [grant number: NCET-11-0826] and the Fundamental Research Funds for the Central Universities [grant number: HEUCF110301].

## REFERENCES

[1] Mamoru Oki, Shuichi Matsumoto, Yoshio Toyoshima, Kazuyoshi Ishisaka and Naoyuki Tsuzuki. 180MPa Piezo Common Rail System. SAE Technical paper series, paper no. 2006-01-0274, April 3-6, 2006, Detroit, U.S.A.

[2] Andrea E. Catania, Alessandro Ferrari, Michele Manno. Development and Application of a Complete Multijet Common-Rail Injection-System Mathematical Model for Hydrodynamic Analysis and Diagnostics. ASME Transactions on Journal of Engineering for Gas Turbines and Power, Vol. 130, No. 062809, 2008, pp.1-13.

[3] Jinwook Lee, Kyoungdoug Min, Kernyong Kang and Choongsik Bae. Hydraulic Simulation and Experimental Analysis of Needle Response and Controlled Injection Rate Shape Characteristics in a Piezo-driven Diesel Injector. SAE Technical paper series, paper no. 2006-01-1119, April 3-6, 2006, Detroit, U.S.A.

[4] Yoshihiro Hotta, Minaji Inayoshi, Kiyomi Nakakita, Kiyoshi Fujiwara and Ichiro Sakata. Achieving Lower Exhaust Emissions and Better Performance in an HSDI Diesel Engine with Multiple Injection. SAE Technical paper series, paper no. 2005-01-0928, April 11-14, 2005, Detroit, U.S.A.

[5] Yi Liu and Rolf D. Reitz. Optimizing HSDI Diesel Combustion and Emissions Using Multiple Injection Strategies. SAE Technical paper series, paper no. 2005-01-0212, April 11-14, 2005, Detroit, U.S.A.

[6] A. Trueba, B. Barbeau, O. pajot and K. Mokaddem. Pilot Injection Timing Effect on the Main Injection Development and Combustion in a DI Diesel Engine. SAE Technical paper series, paper no. 2002-01-0501, March 4-7, 2002, Detroit, U.S.A.

[7] S. Ikezawa, M. Wakamatsu and T. Ueda. Diesel Particulate Analysis Using SEM-EDX and Laser-Induced Breakdown Spectroscopy. International Journal on Smart Sensing and Intelligent Systems.2011, 4:174-188.

[8] Su Han Park, Seung Hyun Yoon and Chang Sik Lee. Effects of multiple-injection strategies on overall spray behavior, combustion, and emissions reduction characteristics of biodiesel fuel. Applied Energy. 2011, 88:88-98.

[9] F. Payri A, Broatch J, M. Salavert and J.Martin. Investigation of Diesel combustion using multiple injection strategies for idling after cold start of passenger-car engines. Experimental Thermal and Fluid Science. 2010, 34:857-865.

[10] G. M. Bianchi, P. Pelloni, F. E. Corcione and F. Luppino. Numerical Analysis of Passenger Car HSDI Diesel Engines with the 2nd Generation of Common Rail Injection Systems: The Effect of Multiple Injections on Emissions. SAE paper 2001-01-1068.

[11] Mirko Baratta, Andrea Emilio Catania and Alessandro Ferrari. Hydraulic Circuit Design Rules to Remove the Dependence of the Injected Fuel Amount on Dwell Time in Multijet CR Systems. ASME Transactions on Journal of Fluids Engineering, Vol. 130, No. 121104, 2008, pp.1-13.

[12] Paolo Lino, Bruno Maione and Alessandro Rizzo. Nonlinear modeling and control of a common rail injection system for diesel engines. Applied Mathematical Modelling. Vol. 31, 2007, pp.1770-1784.

[13] M. F. Russell, G. Greeves and N. Guerrassi. More Torque, Less Emissions and Less Noise. SAE Technical paper series, paper no. 2000-01-0942, March 6-9, 2000, Detroit, U.S.A.

[14] Liyun Fan, Bingqi Tian, Chong Yao, Wenhui Li and Xiuzhen Ma. A study on cycle fuel injection quantity variation for a diesel engine combination electronic unit pump system. Proc IMechE Part A: J Power and Energy. Vol. 226, No. 5, 2012, pp.712-723.

[15] Marco Coppo, Claudio Dongiovanni and Claudio Negri. 2004. Numerical Analysis and Experimental Investigation of a Common Rail-Type Diesel Injector. ASME Transactions on Journal of Engineering for Gas Turbines and Power, Vol. 126, 2004, pp. 874-885.

[16] Ficarella, D. Laforgia and V. Landriscina. 1999. Evaluation of Instability Phenomena in a Common Rail Injection System for High Speed Diesel Engines. SAE Technical paper series, paper no. 1999-01-0192, March 1-4, 1999, Detroit, U.S.A.

[17] D. A. Kouremenos, D. T. Hountalas and A. D. Kouremenos. Development and Validation of a Detailed Fuel Injection System Simulation Model for Diesel Engines. SAE Technical paper series, paper no. 1999-01-0527, March 1-4, 1999, Detroit, U.S.A.

[18] P. Chaufour, G. Millet, M. Hedna, S. Neyrat and E. Botelle. Advanced Modeling of a Heavy-Truck Unit-Injector System and Its Applications in the Engine Design Process. SAE Technical paper series, paper no. 2004-01-0020, March 8-11, 2004, Detroit, U.S.A.

[19] Jose M. Desantes, Jean Arregle and Pablo J. Rodríguez. Computational Model for Simulationof Diesel Injection Systems. SAE Technical paper series, paper no. 1999-01-0915, March 1-4, 1999, Detroit, U.S.A.

[20] G. M. Bianchi, S. Falfari, P. Pelloni, Song-Charng Kong and R. D. Reitz. Numerical Analysis of High-Pressure Fast-Response Common Rail Injector Dynamics. SAE Technical paper series, paper no. 2002-01-0213, March 4-7, 2002, Detroit, U.S.A.

[21] Yuhua Zhu and Rolf D. Reitz. Modeling Fuel System Performance and Its Effect on Spray Characteristics. SAE Technical paper series, paper no. 2000-01-1253, March 6-9, 2000, Detroit, U.S.A.

[22] Qaisar Hayat, Fan Li-yun, Xiu-Zhen Ma and Tian Bingqi. Comparative Study of Pressure Wave Mathematical Models for HP Fuel Pipeline of CEUP at Various Operating Conditions. International Journal on Smart Sensing and Intelligent Systems. 2013, 6:1077-1101.

[23] IMAGINE SA. AMESim User Manual, Version 9.0. 2009.